

184-26527

FINAL TECHNICAL REPORT FOR

NASA GRANT NAG5-126

"A Search for 1) Variability in the UV Spectrum of  $\pi$  Aquarii  
and  
2) Fe III Shell Lines in the Spectra of Be Stars." (\$4600)

Prepared by: Geraldine J. Peters, Principal Investigator  
Department of Astronomy  
Adjunct Assistant Professor  
University of Southern California  
University Park  
Los Angeles, CA 90089

Date: June 22, 1984

During the time interval 1979 January and 1980 December, several short U1 and U2 observations of Be stars were obtained with the Copernicus satellite. These projects included:

- 1) A search for variability in selected UV spectral features in  $\pi$  Aquarii
- 2) A search for Fe III (UV 1) shell lines in the spectrum of the "pole-on" Be star 31 Peg.
- 3) U2 observations of the Si III resonance line  $\lambda 1206$  in  $\mu$  Centauri during its recent active phase.
- 4) Observations of mass flow in the interacting binary Be star HR 2142.

$\pi$  Aquarii (B1 IV-Ve) was observed with the U1 and U2 spectrometers on the Copernicus satellite on 8 June 1979, 15 July 1979, 7 October 1979, and 8 July 1980. These scans were compared with earlier observations on 7 July 1976 and 22 June 1978.

The overall goal of this investigation was to look for variations in the strengths and profiles of selected shell and photospheric features. In order to study possible changes in the temperature of the circumstellar envelope, we observed features covering a wide range in ionization. Included in the observing program were lines of O VI, N V, Si IV, Si III, S III, Fe III, and N I.

We requested four observations of  $\pi$  Aqr which were scheduled at random intervals. Two sets were completed within a five week period to search for shorter term variations. The time interval between the first and the last observation was a year.

The observing program included the following four parts.

- 1) Initially, the Fe III shell lines at  $\lambda 1130$  (UV 1) were scanned with U2. Simultaneously, U1 scanned O VI  $\lambda 1032$ .
- 2) U2 scanned from  $\lambda 1190$ -1210. Spectral features included in this scan are S III (UV 1), Si II (UV 5), N I (UV 1), and Si III (UV 1). U1 scanned Si III (UV 5)  $\lambda 1110$  (one H<sub>2</sub> line is included in this scan) and the region  $\lambda 1030$ -1032 (O VI resonance line and 2 lines each of S II and Si III).
- 3) In this part of the program, U1 scanned from  $\lambda 1128$ -1131 in order to observe the profiles of several Fe III (UV 1) lines. N I  $\lambda 1134$  (UV 2) was also observed to look for shell components and to assess the amount of scattered light in the observational data. U2 covered  $\lambda 1210$ -1250 and included the N V resonance lines,  $\lambda 1239$ , 1243 and the C III line at  $\lambda 1247$  (UV 9).
- 4) The Si IV resonance lines at  $\lambda 1394$  and 1403 were observed with U2 to look for variations in the wind.

The set of observations obtained for this program on 8 June 1979 showed the Fe III (UV 1) lines at  $\lambda 1130$  to be only photospheric. In general, the spectrum near 1130A resembled the first observations of  $\pi$  Aqr in this spectral region (which Theodore P. Snow made in July 1976). However, a scan obtained on 15 July 1979 (one month later) showed the presence of strong Fe III (UV 1) shell lines. This scan resembled the Copernicus scan of the  $\lambda 1130$  region obtained in July 1978. The Copernicus observation of the Fe III (UV 1) lines on 7 October 1979 revealed that the Fe III shell features at 1130A had considerably weakened. No trace of an Fe III shell was observed nine months later on 8 July 1980 (although the S/N

was very low; there were but 10 U1 counts per integration point in the continuum. As evidenced from the profiles of the Si IV resonance lines there was no apparent change in the wind from  $\pi$  Aqr between 8 June 1979 and 15 July 1979. However, the observations in October 1979 revealed a slight enhancement in the wind. Si III  $\lambda$ 1206 showed no variation; O VI was not observed.

Ground-based spectrograms of  $\pi$  Aqr were obtained with the Coude Feed telescope at Kitt Peak National Observatory in June, October, and November 1979. These observations did not reveal the presence of shell structure in the Balmer lines. Therefore, the ground-based spectra appear to be compatible with the UV observations.

The "pole-on" Be star 31 Pegasi was observed with U1 to search for the presence of Fe III (UV 1) shell features. This was motivated by the apparent presence of such lines on a U2 scan from an earlier Copernicus observation in 1974. If confirmed, such an observation would tend to support models for Be envelopes which have a more spherical geometry instead of the flattened geometry which most researchers on Be stars tend to favor for these objects. A total of 47 U1 scans of Fe III  $\lambda$ 1124, 1130 were made and co-added. No shell lines were found.

Soon after ground-based H $\alpha$  observations revealed that the "pole-on" Be star  $\mu$  Centauri had once again developed a circumstellar envelope (Peters, G.J. 1980, I.A.U.C. 3495), Copernicus U2 observations of Si III  $\lambda$ 1206 were scheduled. As seen from Fig. 1, the profile of Si III 1206 appeared identical to an earlier observation obtained during the star's quiescence (15 April 1979) and to one seen in May 1975 (Peters, G.J. 1979, Ap. J. Suppl., 39, 175) when the star displayed moderately strong Balmer emission. These observations have been combined with more recent I.U.E. observations to study the nature of the mass loss and the results are contained in a recent paper (Peters, G.J. 1984, PASP, submitted).

Finally, timed U1 and U2 observations of selected features were completed for the interacting binary Be star HR 2142, (Peters, G.J. 1972, PASP, 84, 334; Peters, G.J. 1983, PASP, 95, 311). From 12 October 1979 - 1 November 1979, four sets of scans (Fe III  $\lambda$ 1130, Si II  $\lambda$ 1264, Si III  $\lambda$ 1206) were obtained throughout the phase interval during which we view the star through its primary and "counter" gas streams.. These observations supplement earlier Copernicus scans. Figure 2 shows the lines of sight of the observations superposed upon our model for the system. Our U1 data reveal that our line of sight cuts into the primary gas stream between phase 0.79 and 0.82 as no significant Fe III, Si II absorption is observed at the earlier phase. Selected Fe III observations are displayed in Figure 3. Note the velocity shift of the feature's centroid relative to the photospheric velocity (shown by the vertical dashed line). This behavior is compatible with the above referenced visual observations (Peters 1983 and references therein). R.S. Polidan and I employed the computer program FITS2 at Princeton University to obtain the density and temperature in the primary gas stream. An example of a theoretical fit to one of the profiles is shown in Figure 4. A fit (solid line) to the 1978 December 5 (phase 0.97) observation (points) is compared with a fit to an earlier observation at the same phase. Note the evidence for secular variability in the gas stream. Combined with IUE observations the Copernicus data suggest a temperature of 19000K and a density greater than  $10^{11}\text{cm}^{-2}$  in the center of the primary gas stream. Other conclusions from this study are:

- 1) The main gas stream in the HR 2142 system is complex; it consists of multiple components. The best fits of theoretical profiles to the observed ones were achieved with the assumption that there are three velocity components in the gas stream.

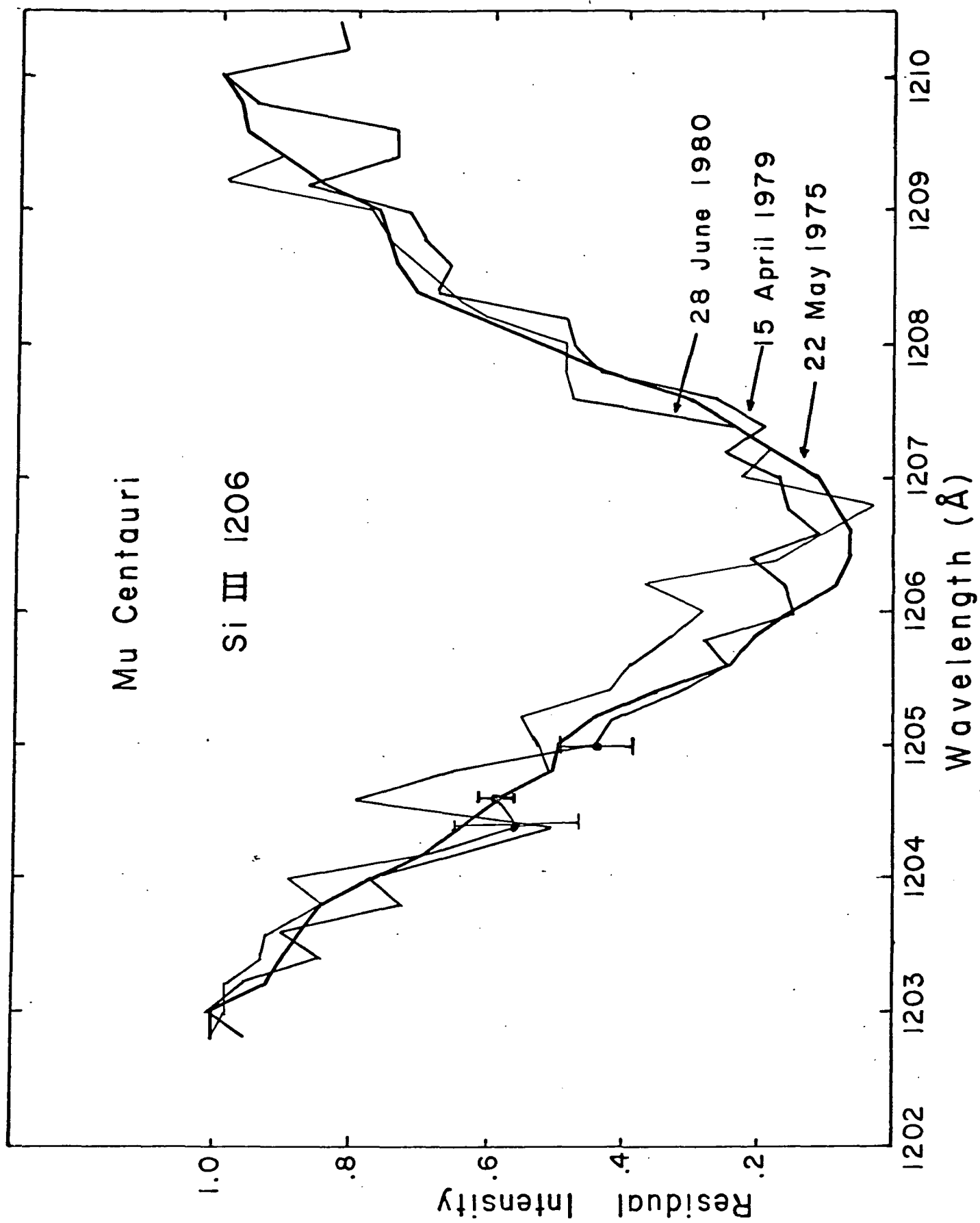
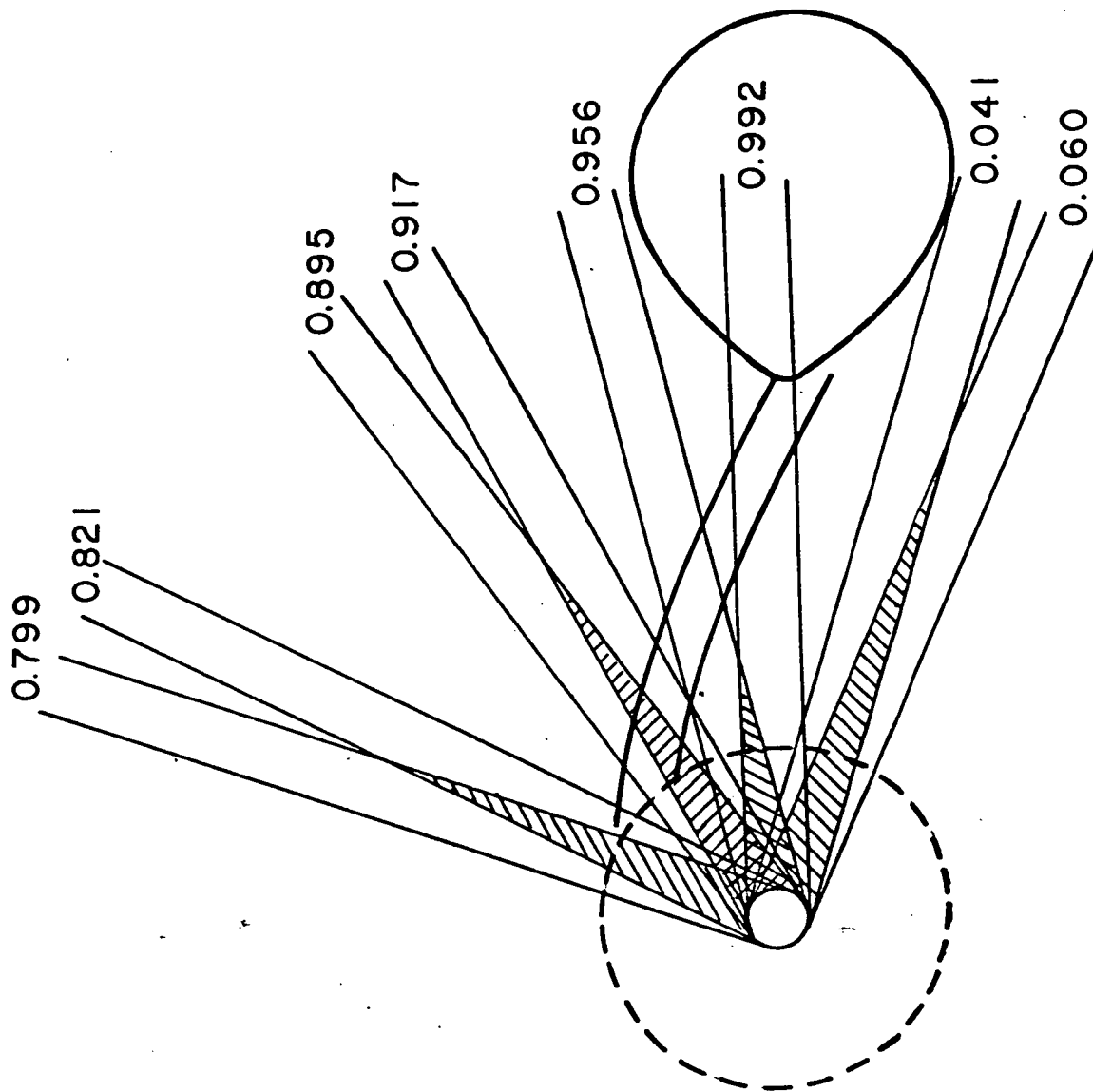


Fig. 1



HR 2142

Fig. 2

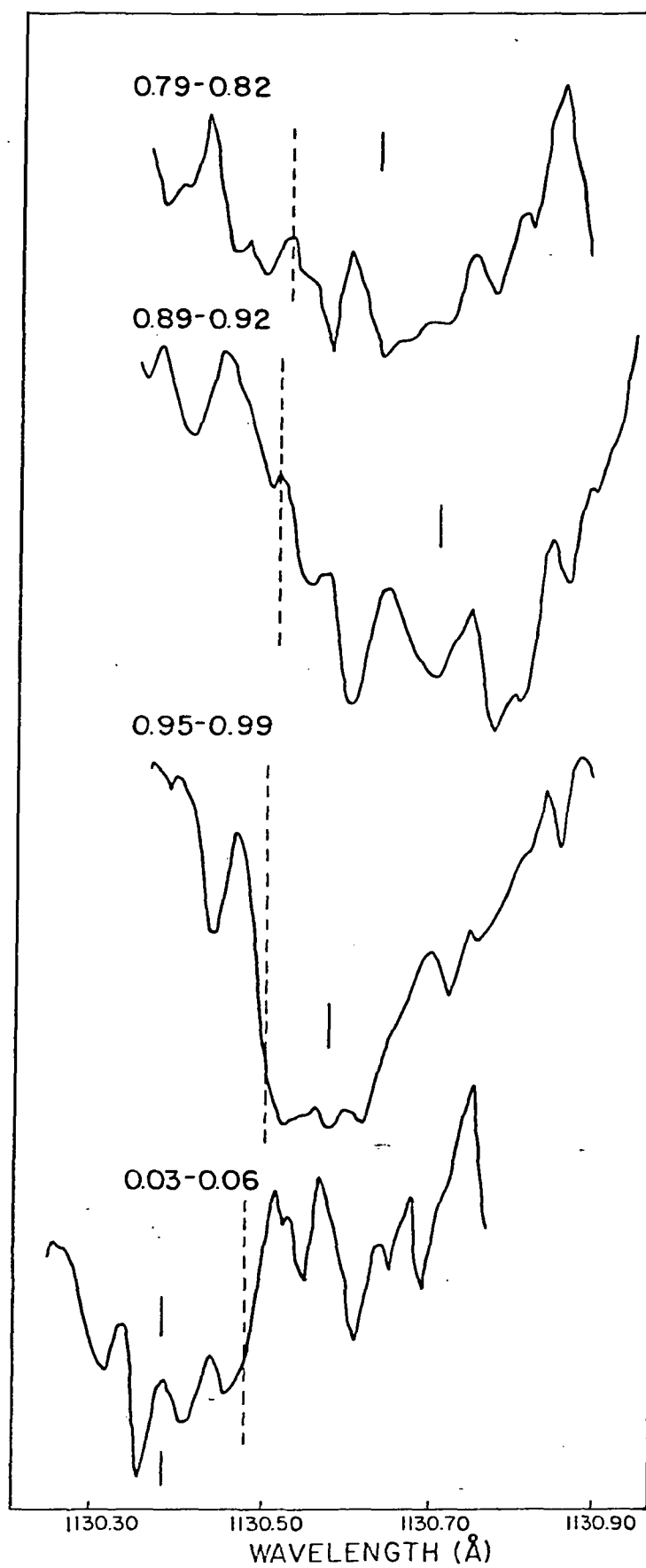


Fig. 3

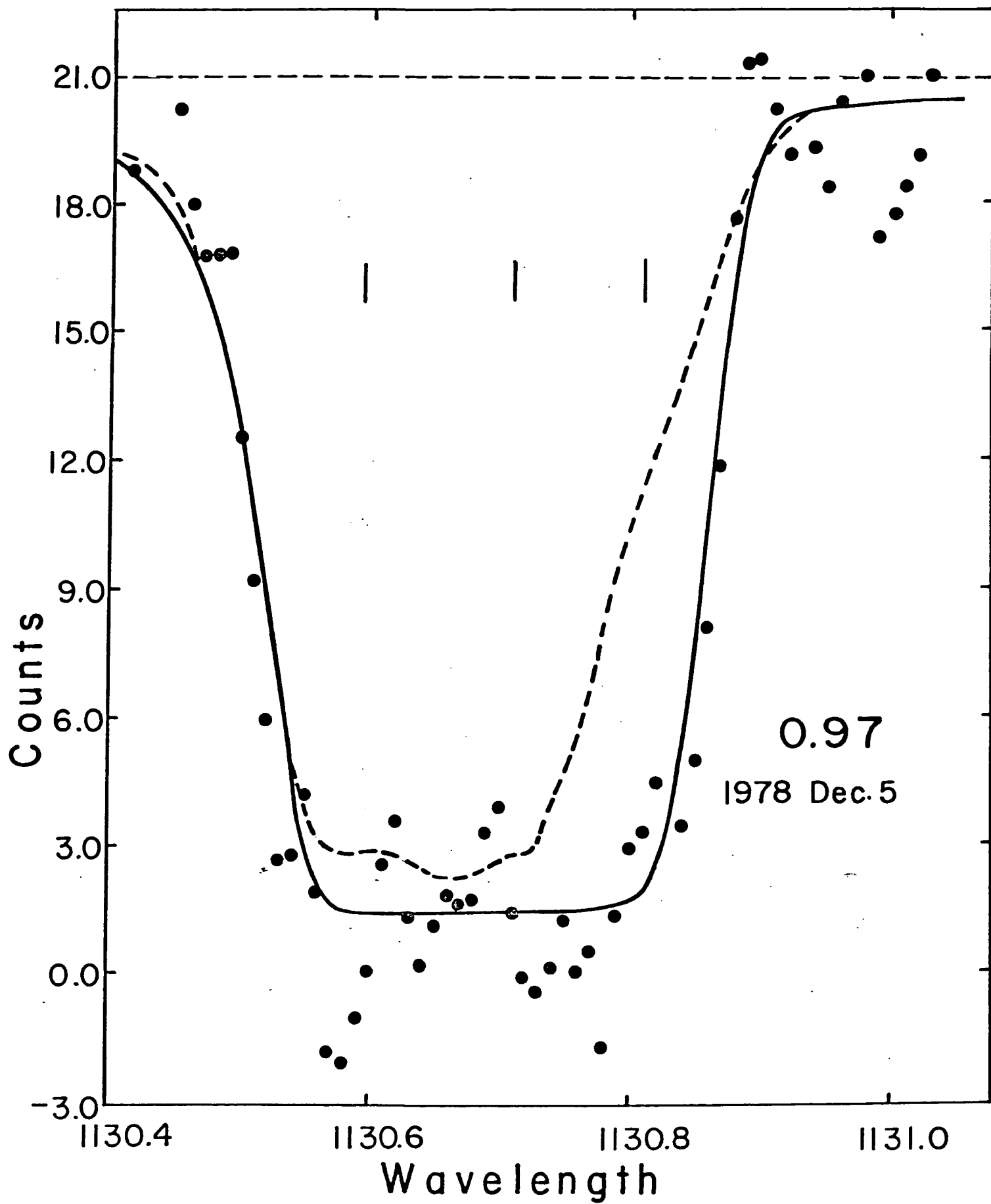


Fig. 4

- 2) The density of the material in the main gas stream is in agreement with theory ( $\rho > 10^{11} \text{ cm}^{-3}$ ).
- 3) The velocity of the streaming material and the angle which the main gas stream makes with the line of centers are not in agreement with theory.
- 4) The structure of the main gas stream has remained stable over the duration of the UV observations (four years).
- 5) Lower density ( $\rho < 10^{11} \text{ cm}^{-3}$ ), higher temperature ( $T=14000^{\circ}\text{K}$ ) material exists at conjunction (no Balmer absorption is observed at this phase).
- 6) Counter-streaming material is present ( $\rho \approx 10^{11} \text{ cm}^{-3}$ ). This gas stream has a large angle with respect to our line of sight ( $i > 80^{\circ}$ ).
- 7) An overall, phase dependent stellar wind is present (it is enhanced near  $\phi = 0.5$ ). A mass loss rate of  $10^{-8} M_{\odot} \text{ yr}^{-1}$  was determined from the profile of Si III 1206.
- 8) A well-defined mass outflow exists between  $0.45 < \phi < 0.5$ . The velocity of this outflowing material is about  $100 \text{ km s}^{-1}$ .

Further details will be given in Peters and Polidan (1984, in preparation).

Results from this project have been published in the following papers of which reprints follow:

- "Ultraviolet Observations of Close Binary Stars" Polidan, R.S., and Peters, G.J. 1980 in Close Binary Stars: Observations and Interpretation (IAU Symposium No. 88), eds. M.J. Plavec, D.M. Popper and R.K. Ulrich, (Dordrecht: Reidel) p. 293-297.
- "Ultraviolet Observations of Interacting Binary Be Stars" Peters, G.J. and Polidan, R.S. 1982, in Be Stars (IAU Symposium No. 98) ed. M. Jaschek and H.G. Groth, (Dordrecht: Reidel), p. 405-409.
- "Orbital Motions and Mass Flow in the Interacting Binary Be Star HR 2142" Peters, G.J. 1983, Publ. A.S.P., 95, 311.
- "On the Presence of OI  $\lambda 1302$  Emission in Be Stars", Oegerle, W.R., Peters, G.J. and Polidan, R.S. 1983, P.A.S.P. 95, 147.



## ULTRAVIOLET OBSERVATIONS OF CLOSE BINARY STARS

R. S. Polidan  
Princeton University Observatory  
Princeton, NJ 08540 USA

G. J. Peters  
Department of Astronomy  
University of Southern California  
Los Angeles, CA 90007 USA

Abstract. In this paper, we present far ultraviolet observations of three interacting binary stars (HR 2142, HR 7084, and  $\lambda$  Tauri). All stars exhibit evidence of a gas stream and extensive mass outflow from the system. Physical parameters are derived for the gas stream in HR 2142.

The physical conditions in the gas streams in close binary systems produce the strongest spectral features in the far ultraviolet. This has made direct study of the mass flow difficult until the advent of satellite astronomy. Observations of three active systems (Table 1) were obtained with the Copernicus satellite during the past two years.

Table 1

### Observations

Star	Components	P(Days)	M <sub>2</sub> /M <sub>1</sub>	Dates of Observation
HR 2142	B1Ve+gK:	80.86	~0.1	Dec. 76 - Feb. 79
HR 7084	B3Ve+F-K	6.70	~0.2	Aug. 78 - May 79
$\lambda$ Tau	B3IV+gA	3.95	0.26	Feb. 78

Selected spectral features between 1000 Å and 1400 Å were investigated at high resolution (0.05 Å) in HR 2142 and  $\lambda$  Tauri and at low (0.20 Å) resolution in HR 7084. Details of the equipment used and technique of observation can be found in Rogerson et al. (1973).

## HR 2142

HR 2142 was suggested to be a mass transfer binary by Peters and Polidan (1973) on the basis of ground based observations. The binary model was refined (Peters 1976) with more observations suggesting a binary with a permanent accretion disk, a thick gas stream, and a counter-stream. The ultraviolet observations were obtained at twelve phase points over seven orbital cycles.

Strong, variable absorption lines, consistent with the existence of a gas stream, were seen in C II, N II, Si II, Si III, S II, S III and Fe III. The gas stream was not detected in lines of C I, C III, N I, N III, O I, and Fe II. Figure 1 shows the phase dependence of the gas stream line strengths normalized to the strength at phase 0.95. The points connected by the solid line was obtained from ground based observations of the hydrogen Balmer lines (Peters 1976). This curve was found to fit the strength variation of the lower ionization (Si II and S II) UV lines. The points with error bars represent the strength variation of the higher ionization species (C II, N II, Si III, S III, and Fe III). Figure 2 shows one of these lines, Fe III 1130.404, at three phases: 0.7 (no stream), 0.95 (peak stream), and 0.02 (counter-stream).

The radial velocity variation of the gas stream lines is shown in Figure 3. Again, the points connected by the solid line were obtained from analysis of ground based data and the low ionization UV lines. The points with error bars represent the velocities of the higher ionization species in the gas stream.

Analysis of the ultraviolet line strengths, velocities, and shapes has yielded three principal results. The gas stream is quite complex. At least two major, repeatable from cycle to cycle, components exist: one producing the higher ionization species and one responsible for the lower ionization species. The slower variation of the higher ionization lines suggests that they are formed in a more extended region than the low ionization lines. Both components appear to be composed of many (>3)

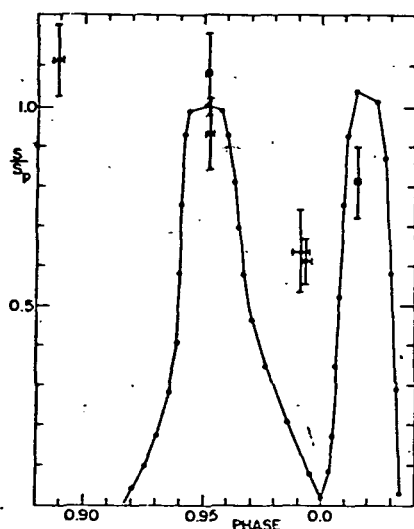


Figure 1. Phase dependence of the gas stream lines in HR 2142.

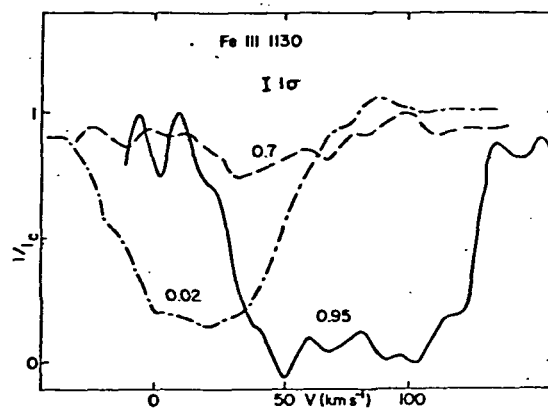


Figure 2. Fe III 1130.404 at three phases in HR 2142.

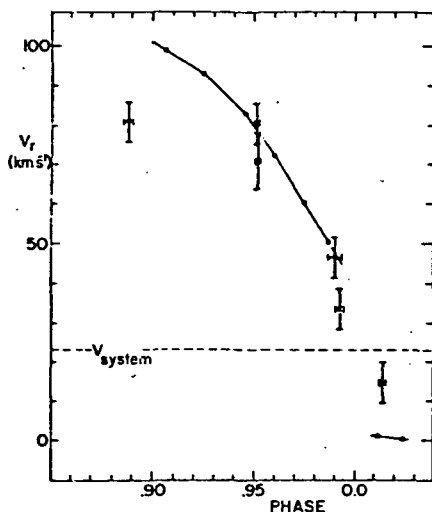


Figure 3. Radial velocity versus phase for the gas stream lines in HR 2142.

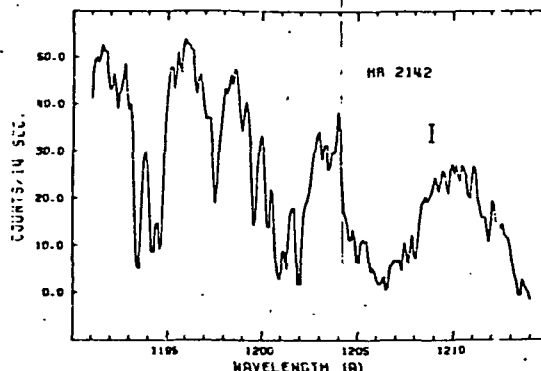


Figure 4. The Si III 1206 region in HR 2142.

discrete "clouds" that do not repeat from cycle to cycle. Analysis of the principal "cloud" in each component suggests that in the higher ionization zone  $T_e \sim 14000$  K and  $N_e \sim 10^{12}$  cm $^{-3}$  and in the lower ionization zone  $T_e \sim 11000$  K and  $N_e \sim 10^{13}$  cm $^{-3}$ . These conditions suggest that the gas stream has a high density "core" and a hot, lower density "halo". The physical conditions discussed above and the model presented earlier (Peters 1976) imply a minimum mass transfer rate of  $10^{-7}$  M $_{\odot}$  yr $^{-1}$  in this system. The final piece of information obtained from the analysis regards the angle at which the gas stream crosses the system. The observed velocity variation (Figure 3) argues in favor of a much greater angle with respect to the line of centers than is predicted by theory (Lubow and Shu 1975). The velocity field is, however, complex. Further analysis and more observation will be required before this deviation can be confirmed.

Observations of HR 2142 at phases when the gas stream is not visible suggest that most of the material that leaves the secondary is ejected from the system and not accreted. In particular, near phase 0.5 negatively displaced ( $V \sim 100$  km s $^{-1}$ ) absorption components, comparable in strength to the strongest gas stream lines are observed. Also, despite the impinging gas stream the rapidly rotating primary star displays a reasonably strong stellar wind at Si III 1206 (Figure 4). Evidence of mass ejection from the system can also be seen in C II 1335 where moderately strong, sharp absorption components not associated with the interstellar medium are seen. The most probable origin of these components is an extensive circumsystem disk or cloud.

Summarizing the results for HR 2142, the physical parameters derived for the gas stream are within the range predicted from theoretical calculations (cf. Lubow and Shu 1975) with the possible exception of the angle the stream makes with the line of centers. Extensive mass outflow from the binary is observed, suggesting that at this stage of evolution

little material is being accreted by the primary star in HR 2142.

#### HR 7084

This Be star has been shown to be an interacting binary star by Koubsky (1978). The ultraviolet observations of this system are less extensive and of lower resolution than those of HR 2142. The general behavior of HR 7084 in the ultraviolet is quite similar to that of HR 2142. A prominent gas stream is seen between phases 0.8 and conjunction and an extensive outflow of material is seen near phase 0.5. The physical conditions in the stream are similar to those found for HR 2142. A strong stellar wind is also seen in the Si III 1206 line of the primary star.

#### $\lambda$ Tauri

The eclipsing binary star  $\lambda$  Tauri has been briefly surveyed at high resolution. A gas stream was detected but at a substantially reduced strength compared to HR 2142 and HR 7084. Similarly, only weak evidence was found for the existence of mass outflow from the system. However, numerous (3 to 6) weak, non-interstellar absorption components were found in C II, N I, and N II, suggesting the presence of multiple circumsystem disks or clouds.

This work was supported by NASA grants NAS 5-23576 (RSP) and NSG 5356 (GJP).

#### REFERENCES

- Koubsky, P.: 1978, Bull. Astron. Inst. Czechosl., 29, pp. 288.  
 Lubow, S. and Shu, F.: 1975, Astroph. J., 198, pp. 383.  
 Peters, G. J.: 1976, in Be and Shell Stars (Ed. A. Slettebak), IAU Symp. No. 70, pp. 417.  
 Peters, G. J. and Polidan, R. S.: 1973, in Extended Atmospheres and Circumstellar Matter in Spectroscopic Binary Systems, IAU Symp. No. 51, pp. 174.  
 Rogerson, J. B., Spitzer, L., Drake, J. F., Dressler, K., Jenkins, E., Morton, D. C., and York, D. G.: 1973, Astroph. J., 181, pp. L97.

# ULTRAVIOLET OBSERVATIONS OF INTERACTING BINARY Be STARS

Geraldine J. Peters  
Department of Astronomy, Univ. of Southern California  
Los Angeles, CA 90007 USA

Ronald S. Polidan  
Princeton University Observatory  
Princeton, NJ 08540 USA

## ABSTRACT

Initial results from the analysis of a series of timed, high resolution IUE observations of HR 2142,  $\phi$  Per, CX Dra, KX And, AU Mon, and TT Hya are presented. The data base for HR 2142 also includes Copernicus U1 and U2 observations. Variable absorption lines, indicative of mass flow in the system, are observed in all objects except  $\phi$  Per. We also, in general, find evidence of mass outflow in the form of winds and/or discrete components. We observe variable N V absorption in CX Dra and AU Mon and emission features in KX And and  $\phi$  Per (C IV only). U1 data reveals the presence of complex structure in the gas stream in HR 2142. These observations are compared with those of Be stars which are not thought to be interacting binaries.

## 1. INTRODUCTION

The ultraviolet spectra of interacting binary Be stars contain a wealth of data on the gas streams, general matter flow, and disks in these systems. In this paper, we present the initial results from a detailed study of the UV spectra of some of the brighter systems. The properties of the program stars and the phases at which the observations were obtained are given in Table 1. All IUE observations were made from 1979 October 23 to 1981 February 25. Copernicus observations of HR 2142 were from 1976 December to 1979 December.

## 2. RESULTS

### a. HR 2142

Evidence that HR 2142 is an interacting binary and the behavior of the visible "gas stream" lines throughout the observed two-component shell phase are given in Peters (1976) and the references quoted therein. Orbital parameters for the system (which lend support to the proposed model) are included in Peters (1982). Striking phase dependent spectral variations have also been observed in the far ultraviolet (Peters 1981, Paterson-Beeckmans 1980, Polidan and Peters 1980). Some UV gas stream lines include the resonance lines of C II, Mg II, Al II,

Table 1 - The Program Stars

Stars	Sp Types	Period	Phase coverage
HR 2142	B1IV-Ve+?	80. <sup>d</sup> 860	IUE ( $0.8 < \phi < 0.1$ : 11 obs. + $\phi = 0.17, 0.42, 0.45, 0.47$ ) <u>Copernicus</u> ( $0.8 < \phi < 0.1$ : 14 obs. + $\phi = 0.30, 0.44, 0.49, 0.70$ )
$\phi$ Per	B0IV-Ve+?	126. <sup>d</sup> 696	0.00, 0.22, 0.25, 0.46, 0.46, 0.66, 0.85
CX Dra (HR 7084)	B3Ve+?	6. <sup>d</sup> 697	0.40, 0.56, 0.57, 0.60, 0.83, 0.86, 0.90
KX And (HD 218393)	B3IVe+K1III	38. <sup>d</sup> 9	4 obs., 3 close in phase, one 0. <sup>p</sup> 6 later ( $\phi$ arbitrary)
AU Mon (HD 50846)	B5Ve+F	11. <sup>d</sup> 113	0.30, 0.48, 0.85, 0.93
TT Hya (HD 97528)	B9Ve+G5	6. <sup>d</sup> 953	0.40, 0.90

Al III, Si II, III, IV, S II, III, Ti III, and Fe III and numerous subordinate lines of Fe III and Si III. In general, the variations in the strengths and velocities of the UV features parallel those observed in the visible. However, there are some important differences. The UV "shell phase" or gas stream phase persists from  $0.80 < \phi < 0.10$ . Gas stream features are observed prior to the visible primary shell phase, at conjunction, and after the short-termed visible secondary shell phase. IUE observations reveal that the absorbing stream and/or disk cuts into the line of sight abruptly between  $0.83 < \phi < 0.86$ . During this interval of time, many of the stronger resonance lines saturate. The strengths of the gas stream lines remain fairly constant between  $0.90 < \phi < 0.95$ . Then, from  $0.95 < \phi < 0.97$ , there is an additional strengthening of the UV gas stream lines which coincides in time with the appearance of the conspicuous Balmer shell spectrum ( $\phi_s \approx 0.0$ ). The features subsequently weaken; at conjunction the column densities are about 100 - 150 times lower than the values observed from  $0.91 < \phi < 0.96$ . We further observe a strengthening of the gas stream lines after conjunction (coincident with the visible secondary shell phase) and the column densities from these features are comparable with those obtained from the lines observed during the primary shell phase. The UV gas stream lines disappear by  $\phi = 0.10$ .

A detailed line profile analysis of Copernicus U1 observations of the Fe III 1130 Å resonance line has clearly shown that the gas stream features are complex. Each line is composed of at least 2 - 3 components, one of which yields a column density 100 times greater than the others. The denser component (at  $\phi = 0.91, 0.96$ , and  $0.03$ ), which appears to be fixed in velocity prior to conjunction ( $V - V_{\text{hot}} = 30 \text{ km}^{-1}$ ), suggests a column density (in 1130 only) of about  $10^{18} \text{ cm}^{-2}$ . If the path length is about  $10R_\odot$ , then the latter value implies a particle density in excess of  $10^{12} \text{ cm}^{-3}$ . The velocity shifts of the weaker 1130 components (at  $\phi = 0.91, 0.96$ ) are more in accordance with those from the Balmer lines.

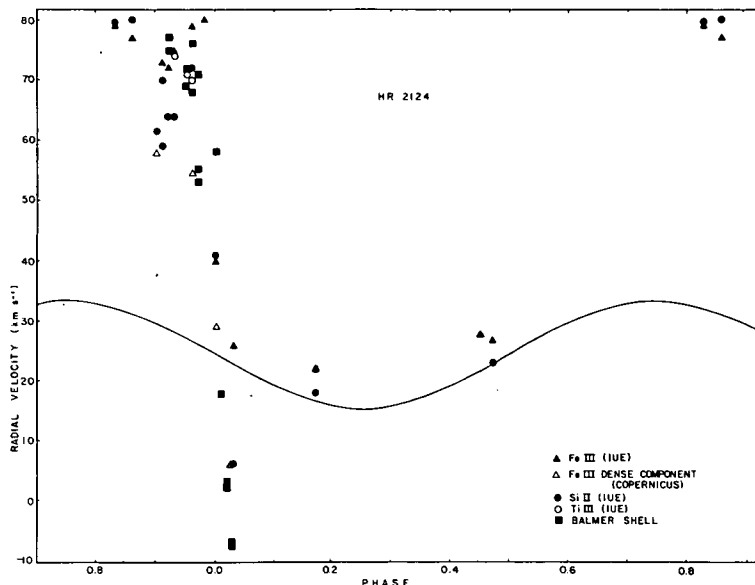


Fig. 1 - Radial velocities from selected gas stream lines versus phase. The solid curve shows the motion of the primary.

The radial velocity data from various gas stream features is summarized in Figure 1. Note that without exception the motion of the absorbing matter is toward the photosphere before conjunction; the opposite is observed after conjunction. However, if the lines are indeed formed in a conventional gas stream and counter stream, the velocities are significantly lower than theory predicts. Perhaps, the streams have large inclinations with respect to the line of centers or we are simply viewing through a density enhancement in the disk which results from a stream/disk interaction. Many resonance lines show evidence of outflow in discrete components near  $\phi = 0.5$  (Paterson-Beeckmans 1980). Our observations suggest that this outflow phase peaks at  $\phi \approx 0.45$  (before  $L_3$ ). Subordinate lines do not show the outflow (cf. Fig. 1). We also observe an overall stellar wind (in C IV, Si III, IV) which appears to be enhanced at conjunction.

#### b. $\phi$ Perseid

An orbit and model for this enigmatic binary have recently been published by Poeckert (1981). Whereas striking phase dependent spectral variations are observed in the visible, our IUE observations show this star to be relatively invariant in the UV (unlike HR 2142). With one exception, the UV spectrum of  $\phi$  Per is typical for a Be-shell star. The C IV resonance doublet stands as unique, however. As shown in Fig. 2, the C IV lines have P Cygni profiles with a peak emission line strength of twice the continuum value. Of the twenty-five classical Be stars observed to date with IUE, only  $\phi$  Per displays C IV emission. Perhaps even more novel is that we do not observe emission at N V or Si IV. Our IUE observations were obtained over four orbital cycles and, in general, no statistically significant profile variations were observed.

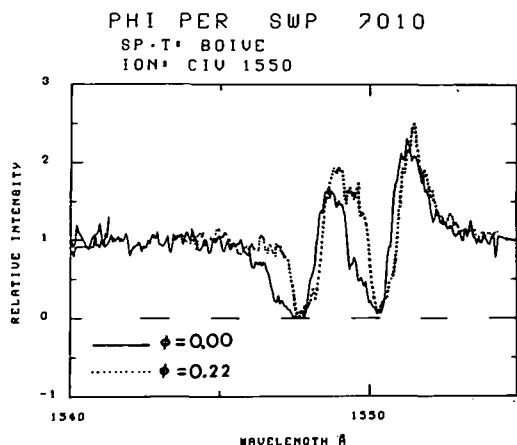


Fig. 2 - The resonance lines of C IV in  $\phi$  Per at two phases.

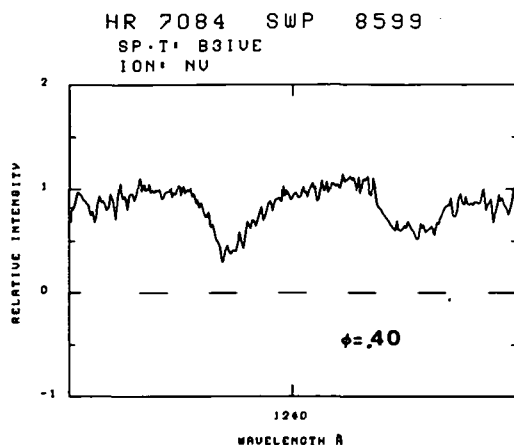


Fig. 3 - The N V resonance lines in CX Dra on 1980 March 30.

In order to determine whether the C IV feature is associated with the proposed high temperature secondary (Poeckert 1981), radial velocities were measured for the C IV doublet using neighboring interstellar lines for wavelength calibration. Reference points on the profile included the emission line peak and wings and the cores of the lines. The data clearly show that the feature is associated with the primary. Within the uncertainties of the measurements, the motion of the C IV region follows the radial velocity curve of the primary. Motion with respect to the secondary would be quite conspicuous since  $K_s = 100 \text{ km s}^{-1}$ . Possibly the only observed UV features associated with H $\delta$  II object (secondary) are redshifted cores to Si III (UV 4) observed at  $\phi = 0.66$ .

#### c. CX Draconis (HR 7084)

Koubsky (1978) proposed that this object is a mass transfer binary system. IUE observations reveal redward displaced absorption components, indicative of a gas stream, in the resonance lines of C II, Si II, III, IV, and Al III and the subordinate lines of Fe III at  $\phi = 0.83, 0.86$ , and  $0.90$ . These features are broader than their counterparts in HR 2142 and show a larger velocity shift from the photospheric lines ( $V = 200\text{--}250 \text{ km s}^{-1}$ ). We also observe violet asymmetries in the above mentioned lines at  $\phi = 0.56, 0.57$ , and  $0.60$  which suggest the presence of mass loss.

Quite unexpected was the discovery of strong N V features in the spectrum of this "B3e" star (Fig. 3). Under normal circumstances, a temperature of at least 40000K is required to form N V. The strength of the N V doublet is quite variable ( $0.25 < r_v < 0.95$ ) but does not appear to be phase dependent. Since the radial velocities from the N V lines apparently follow Koubsky's published radial velocity curve, we conclude that the N V is formed close to the stellar photosphere (perhaps the result of an impacting gas stream). Plavec (personal communication) recently has found CX Dra to be a soft X-ray source. We suggest that the X-rays and N V both arise in an accretion heated region near the primary.



## d. KX Andromedae (HD 218393)

Observations of this system at essentially two different phases ( $\Delta\phi = 0.6$ ) reveal the presence of broad emission at the resonance lines of C II, Si IV, Al III, and Mg II. Numerous shell lines which vary in strength and width, pervade the UV spectrum. The IUE data support the spectral classification of B2 (Doazan and Peton 1970).

## e. AU Monocerotis (HD 50846)

If AU Mon were not an eclipsing binary, it would be considered an average B5e star. IUE observations show this system to be quite similar to CX Dra. A similar gas stream is seen ( $\phi = 0.85, 0.93$ ) and equally strong, variable N V (and C IV) resonance lines are found.

## f. TT Hydrae (HD 97528)

TT Hya is a well-known Algol-type eclipsing binary. The prominent H $\alpha$  emission feature observed in this system displays phase dependent V/R variations (Peters 1980). A rich shell spectrum, which does not appear to be highly variable, is seen in the UV. The gas stream was detected in the resonance lines of C II and Si II.

## 3. DO THE UV SPECTRA OF INTERACTING BINARY Be STARS DIFFER FROM THOSE OF "SINGLE" Be STARS?

IUE observations of six Be stars which are known to be mass transfer binaries have, unfortunately, not revealed a single spectral feature, set of features, or spectroscopic behavior which alone can be considered a signature of an interacting system. However, there are a number of criteria which can be employed to find possible binaries. These include the presence of 1) numerous shell lines, especially those which arise from low lying and/or metastable levels, 2) redward asymmetries in the resonance features, and 3) variable N V absorption. Normally, N V features are not observed in Be stars later than B1 (Marlborough and Peters 1982) but, among our program binaries, we have observed strong N V as late as B5!

We gratefully acknowledge support from NASA grants NSG 5422, NSG 5356, NAG-5-126 (GJP), and NAS 5-23576 (RSP).

## REFERENCES

- Doazan, V., and Peton, A.: 1970, *Astron. Astrophys.* 9, pp.245-251.  
 Koubsky, P.: 1978, *Bull.Astron.Inst.Czech.* 29, pp.288-298.  
 Marlborough, J.M., and Peters, G.J.: 1982, this volume, pp.387-390.  
 Paterson-Beeckmans, F.: 1980, *Proc.Sec.European IUE Confer.*, pp.51-54.  
 Peters, G.J.: 1976, in 'Be and Shell Stars', IAU Symposium 70, pp.417-428.  
 Peters, G.J.: 1980, in 'Close Binary Stars: Observation and Interpretation', IAU Symposium 88, pp. 287-292.  
 Peters, G.J.: 1981, in 'The Universe at Ultraviolet Wavelengths: The First Two Years of IUE', NASA publ., in press.  
 Peters, G.J.: 1982, this volume, pp.311-314, 353-357, 401-404, 411-414.  
 Poeckert, R.: 1981, *Publ.Astron.Soc.Pacific*, 93, in press.  
 Polidan, R.S., and Peters, G.J.: 1980, in 'Close Binary Stars: Observations and Interpretation', IAU Symposium 88, pp. 293-297.

# ORBITAL MOTION AND MASS FLOW IN THE INTERACTING BINARY Be STAR HR 2142

GERALDINE J. PETERS

Department of Astronomy, University of Southern California, Los Angeles, California 90089

Received 1982 August 4, revised 1983 February 7

An orbital solution based upon the measurements of the wings of the broad Balmer and He lines is presented for the Be star HR 2142. Parameters for this 80<sup>d</sup>860 binary include:  $K = 9.4 \text{ km s}^{-1}$ ,  $V_0 = 24.1 \text{ km s}^{-1}$ , and  $f(M) = 0.007 M_\odot$ . If the mass of the primary is  $11 M_\odot$ , then the secondary is a one-solar-mass object. This solution confirms an earlier suggestion that the unusual two-component, periodic shell phase observed in this system is due to mass transfer. Mass flow in the Balmer-line-formation region is also discussed and a model for the system is suggested.

*Key words:* interacting binary systems—Be stars—stars: individual

## I. Introduction

The discovery of an unusual, periodic, two-component shell phase of short duration in the "classical" Be star HR 2142 (HD 41335, MWC 133) offered convincing evidence that this object is a mass-transfer binary system (Peters 1971, 1972, 1976). A model based solely on the phase-dependent behavior of the hydrogen shell lines in this 80<sup>d</sup>860 binary was developed (Peters and Polidan 1973; Peters 1976) using a system of phases measured from the time of maximum Balmer core strength during the *primary* shell phase. Following earlier terminology, the *primary* shell phase is the first segment of the two-component shell phase while the second part is referred to as the *secondary* shell phase. Balmer core strengths are comparable during both shell phases (spaced about five days apart) but the duration of the primary shell phase (seen in the visible spectrum) is about six days and the lines are red-shifted relative to the photosphere while the secondary shell phase lasts only 1<sup>d</sup>5 with the Balmer cores blue-shifted relative to the photosphere.

In this paper, a refinement to the earlier model for this system is presented utilizing an orbital solution obtained from measurements of the wings of the broad photospheric features observed in the rapidly rotating primary. Velocities and equivalent widths from the sharp "shell" lines, presumably formed in or near the gas stream, provide additional information on the mass flow in the Balmer-line-formation region.

## II. Observations and Plate Measurements

The data used for this investigation are spectrograms of reciprocal dispersion  $11 \text{ \AA}$  or  $16 \text{ \AA mm}^{-1}$  (widened 0.6–1.0 mm on the plate) obtained with the coude spectrograph of the 3-m Shane telescope at Lick Observatory. Plates from both the main telescope and the 61-cm coude auxiliary telescope were utilized but observations from the larger telescope were generally given higher weight. Table I contains the journal of all observations

considered in this analysis. The quoted phases in the second column come from the orbital solution;  $\Phi_s$  are the phases used in the earlier study and defined above. The remainder of the data in the table are from the plate measurements and orbital solution.

The photospheric features in the spectrum of HR 2142 are rotationally broadened ( $v \sin i = 350\text{--}400 \text{ km s}^{-1}$ ; Peters 1972, Slettebak 1976, 1982) to the extent that only the lines of hydrogen and helium are deep enough to be accurately measured. Furthermore, all of the Balmer lines and some of the helium features have complex emission-line cores. Therefore, only the wings of these broad features can be used to obtain the position of the centroid of the line. In order to successfully carry through these difficult measurements, the wide-scan oscilloscopic comparator at the Dominion Astrophysical Observatory (ARCTURUS) was employed. The lines which produced the most reliable measurements and were generally included in the determination of the mean photospheric velocity for a particular observation are: H $\delta$ , H8, H9, H10, H11, and He I  $\lambda\lambda 4144, 4026, 4009$ , and  $3820$ . H $\gamma$  was excluded because it is blended with numerous O II lines on its red wing and it is also positioned on the far edge of the plate where the decline in exposure is significant. Both combine to render the H $\gamma$  measurements artificially high and introduce a false red-shift. He was excluded because it is blended with He I  $\lambda 3964$  (yields systematic negative velocity) while the measurements of He I  $\lambda 4388$  were not considered because the feature is blended with an Fe II emission line.

## III. Orbital Solution

The final orbital solution was carried through assuming that the period is 80<sup>d</sup>860 and the orbit is circular. Orbital parameters are listed in Table II and a plot of this solution is presented in Figure 1. All the parameters in Table I have their usual meaning except that  $T$  is the epoch of conjunction. The phase difference between this

TABLE I  
JOURNAL OF THE OBSERVATIONS

J.D. (2440000+)	Phase <sup>1</sup>	$\phi_s$ <sup>2</sup>	Radial <sup>3</sup> Velocity (km s <sup>-1</sup> )	$\sigma$ <sup>4</sup> (km s <sup>-1</sup> )	O-C <sup>5</sup> (km s <sup>-1</sup> )	Weight
520.03	0.81	0.85	35.6	$\pm$ 6.0	2.9	1.0
527.05	0.90	0.94	35.3	12.2	5.7	0.7
544.94	0.12	0.16	20.2	14.0	2.6	1.0
572.94	0.47	0.51	26.4	23.3	4.2	0.3
611.80	0.95	0.99	28.4	13.4	1.3	1.0
637.73	0.27	0.31	16.0	7.0	1.2	1.0
638.63	0.28	0.32	14.7	16.0	- 0.2	0.7
659.61	0.54	0.58	24.3	15.9	- 2.1	1.0
850.04	0.89	0.93	33.7	10.7	3.8	1.0
877.96	0.24	0.28	20.4	11.6	5.6	1.0
903.92	0.56	0.60	34.3	4.5	6.7	1.0
932.84 <sup>6</sup>	0.92	0.96	43.6	19.7	15.0	0.1
996.68	0.71	0.75	36.5	11.0	3.4	0.7
1200.04	0.22	0.26	13.4	14.7	- 1.5	1.0
1228.06	0.57	0.61	27.0	14.0	- 1.1	1.0
1236.04	0.67	0.71	39.0	9.6	6.7	1.0
1256.98	0.93	0.97	27.6	9.5	- 0.6	1.0
1256.98	0.93	0.97	30.0	8.4	1.8	1.0
1261.00	0.98	0.01	26.1	6.2	0.64	1.0
1261.00	0.98	0.01	20.7	10.7	- 4.8	1.0
1346.70	0.04	0.07	23.3	8.2	1.3	1.0
1346.70	0.04	0.07	20.8	11.3	- 1.2	1.0
1374.67	0.38	0.42	13.8	19.3	- 4.0	1.0
1404.62	0.75	0.79	34.5	12.8	1.0	1.0
1406.63	0.77	0.82	29.2	10.3	- 4.1	1.0
1433.65	0.11	0.15	13.0	17.0	- 5.0	1.0
1590.04	0.05	0.08	17.4	6.5	- 4.0	1.0
1591.00	0.06	0.10	18.7	14.1	- 2.1	1.0
1614.94	0.35	0.39	16.5	18.0	- 0.2	1.0
1616.96	0.38	0.42	13.1	18.4	- 4.6	1.0
1643.98	0.71	0.75	28.8	11.1	- 4.4	1.0
1644.89	0.72	0.76	25.9	11.3	- 7.5	1.0
1644.90	0.72	0.76	28.3	12.0	- 5.1	1.0
1987.02	0.96	0.99	19.0	8.5	- 7.7	0.7
1987.97	0.97	0.01	29.5	8.6	3.5	0.7
1936.02	0.33	0.36	12.9	6.9	- 2.9	1.0
1975.00	0.81	0.84	31.4	25.0	- 1.5	0.3
1990.95	0.00	0.04	27.3	16.7	3.4	1.0
1991.90	0.02	0.05	22.6	18.0	- 0.6	1.0
1992.07	0.02	0.06	22.8	14.5	- 0.3	1.0
2036.87	0.57	0.61	27.7	35.9	- 0.5	0.3
2083.73	0.15	0.19	15.3	14.5	- 1.2	1.0
2149.65	0.97	0.00	23.4	6.9	- 2.6	1.0
2312.02	0.98	0.01	18.5	8.8	- 7.1	0.1
2316.97	0.04	0.07	30.9	8.9	8.9	1.0
2317.03	0.04	0.07	24.2	11.1	2.2	1.0
2317.98	0.05	0.09	24.2	9.0	2.9	1.0
2317.98	0.05	0.09	22.5	11.3	1.2	1.0
2318.97	0.06	0.10	15.9	3.5	- 4.7	1.0
2682.01	0.55	0.59	32.9	17.9	5.8	1.0
2733.94	0.19	0.23	19.4	24.0	4.1	0.7

<sup>1</sup> Measured from inferior conjunction (primary star in back)

<sup>2</sup> Phase based upon strengths of gas stream lines (Peters 1976)

<sup>3</sup> Photospheric velocity

<sup>4</sup> Standard deviation of an individual observation

<sup>5</sup> Residuals from adopted orbital solution

<sup>6</sup> Given low weight because absorption in gas stream significantly affected measurements of photospheric lines

TABLE II  
ORBITAL PARAMETERS FOR HR 2142

$P = 80.860 \pm .005$ days
$T = \text{JD } 2441990.5 \pm 1.1$
$e = 0$
$V_o = 24.1 \pm 0.6 \text{ km s}^{-1}$
$K = 9.4 \pm 0.9 \text{ km s}^{-1}$
$f(m) = 0.007 \pm 0.002 M_\odot$
$a \sin i = 1.04 \times 10^7 \pm 0.10 \times 10^7 \text{ km}$
$\phi_s - \phi = 0.035$

quantity and the earlier epoch of maximum core strength during the *primary* shell phase ( $\Phi_s$ ) is also given.

It appeared reasonable to adopt the period determined from timing the shell phases because of the strict periodicity of these phases and the long baseline between the earliest known shell-phase observation and the present. Perhaps the most valuable spectrogram for assessing the uncertainty in the period is the University of Michigan plate taken on 1933 October 6 (cf. Peters 1972). Inspection of this plate reveals the presence of strong Balmer cores which indicate a phase of  $0.00 \pm 0.02$  for the observation. Of course, the low dispersion of the plate prevents us from ascertaining whether the observation was made during *primary* or *secondary* shell phase, but odds are in favor of the former because its duration is four times that of the latter. Since 225 cycles have elapsed between the 1933 observation and the present, an uncertainty of about 1.5 days in the phase of the earlier observation indicates an uncertainty of  $0.007$  in the period. The newer observations can be used exclusively to assess the error in the period if one considers the timing of the *secondary* shell phase. About 45 cycles have been completed since we obtained the first Lick Observatory spectrogram identified as having been taken during the peak of the *secondary* shell phase. As the onset of the *secondary* shell phase can now be predicted with an uncertainty of less than  $0.025$ , the implied uncertainty in the period is  $0.005$ . It should be noted that a period of  $80.860$  predicts precisely the same phase for two *secondary* shell phase observations taken twelve cycles apart (JD2441346.7 and JD2442317.0, respectively). An orbital solution in which the period was allowed to vary suggested a period of  $80.808$  but this period was ruled out because it predicted phases nearly a day apart for the above mentioned *secondary* shell-phase observations.

The adoption of a circular orbit was preferred over a solution in which the eccentricity was allowed to vary

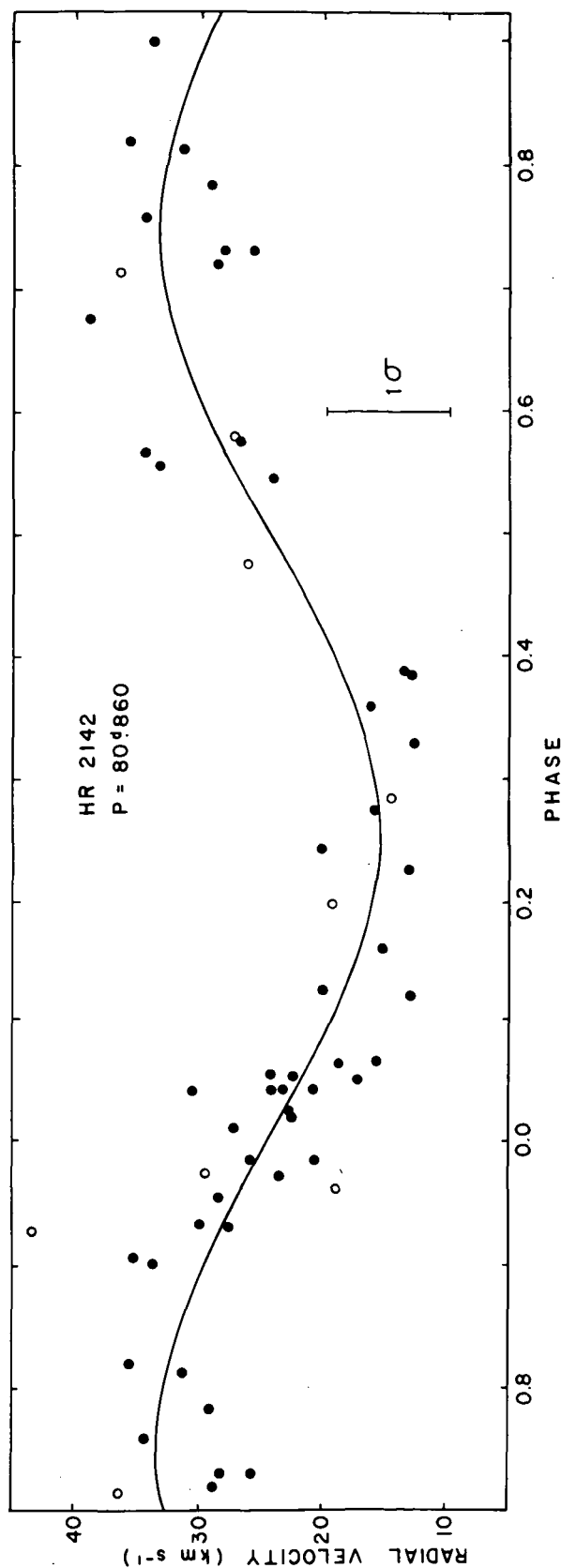


FIG. 1—Radial-velocity curve and individual observations for HR 2142. Observations indicated by the open circles were given lower weight in the analysis. The error bar represents a typical standard deviation from a single plate.

because gas streaming effects cause one to measure an artificially large velocity near phase 0.9. Finally, there did not appear to be a statistically significant difference between the orbital solution based solely upon either the hydrogen or helium lines. In view of the fact that the standard deviation from a single plate was comparable to the semiamplitude of the orbit, one appears justified in considering all the measurable hydrogen and helium lines collectively.

#### IV. Mass Flow in the Circumstellar Matter

The sharp, Balmer "shell" lines observed during the *primary* and *secondary* shell phases are most assuredly formed in domains of mass flow in the system. In fact, in more recent papers on HR 2142, these features have been called "gas stream" lines since the inferred geometry of the region in which these lines are formed appears to be complex and asymmetrical and does not resemble a spherical shell in the least. Nevertheless, since the term "shell line" implies the presence of a relatively narrow

absorption feature formed above the photosphere, the term remains appropriate for the sharp features periodically observed in HR 2142.

In order to learn more about the mass flow in this system, the sharp Balmer cores and the equally narrow features of He I  $\lambda\lambda 3889, 3964$ , and  $5015$ , were measured on all plates on which they were observed. The results are listed in Table III and displayed in Figure 2. In Table III, the velocities from H $\beta$ -H $\delta$  are listed separately as well as the velocities from He I  $\lambda 3889$  and the mean from all observable Balmer cores excluding H $\beta$ .

The earliest phase at which Balmer-shell features are observed is 0.895; cores in the higher Balmer lines are not observed until phase 0.925. The sharp Balmer and He I features reach maximum strength at a phase of 0.965 then begin a rapid decline in strength as the stars approach conjunction. An H $\beta$  core is *barely* detectable at conjunction. The Balmer- and He I-shell features return briefly to their previous strength during the short-lived *secondary* shell phase. As mentioned above, the ve-

TABLE III

RADIAL VELOCITIES FROM GAS STREAM LINES

Plate Number (EC/EP)	Phase	H $\beta$	H $\gamma$	H $\delta$	He I (3889) <sup>1</sup>	$\overline{V}^2$ (km s <sup>-1</sup> )	Notes
8866	0.895	97.5					4
8867	.895	87.7					4
8110	.900	75.5	61.3			61.3	3,4
9174	.921	89.0	101.5:			101.5:	3,4
9999a	.927	83.3	73.6	75.6	76.0	75.1 $\pm$ 1.3	
9999b	.927	77.3	71.9	80.2	80.9	77.7 $\pm$ 5.0	
8306	.948	74.8	73.9	71.4	93.0	68.8 $\pm$ 4.9	
2585	.956		68.1	70.2	98.9	72.0 $\pm$ 6.7	5
2600	.966		67.6	70.5	89.5	67.9 $\pm$ 8.7	5
12273	.967		77.8	78.3	97.3	76.0 $\pm$ 7.8	5
3789	.976		72.2	72.0	89.5	76.0 $\pm$ 5.7	5
10010	.977	49.8	51.7	54.9	51.9	55.4 $\pm$ 5.3	
10011	.977	53.1	51.7	59.1	53.0	53.3 $\pm$ 2.2	
3801	.988		68.0	73.2	79.4	70.6 $\pm$ 3.7	5
11919	.004	23.6	58.0			58.0	3,4
11928	.016	39.5	18.3			18.3	3,4
11940	.018	42.4	42.6			42.6	3,4
12713	.036	11.4	4.8	7.2	5.2	3.0 $\pm$ 3.4	
12715	.037	8.8	3.4	3.6	6.1	1.7 $\pm$ 2.0	
10172a	.037	2.4	-3.2	-3.6	-2.9	-6.8 $\pm$ 3.2	
10172b	.037	-0.6	-4.1	-7.2	-1.9	-6.8 $\pm$ 2.6	
10177	.039	1.6					6
10178	.039	4.6					6
10179a	.039	0.9					6
10179b	.039	5.0					6
10984	.046	25.0	26.0		1.5	26.0	3,4
12733	.049	17.4	14.3	0.0	7.1	7.1 $\pm$ 7.0	3,4
12734	.049		9.7	10.2	5.9	10.0 $\pm$ 0.5	3,4
10990	.058	22.1					4
12745	0.061	45.3					4

1 Contamination with H $\gamma$  from  $0.95 < \phi < 0.98$  and  $0.03 < \phi < 0.04$ .

2 Average velocity from H $\gamma$  through higher Balmer lines.

3 H $\gamma$  only or H $\gamma$  and H $\delta$ , only considered for average velocities.

4 Cores not present in higher Balmer lines.

5 Data quality at H $\beta$  region poor.

6 Higher Balmer lines not measured - low data quality.

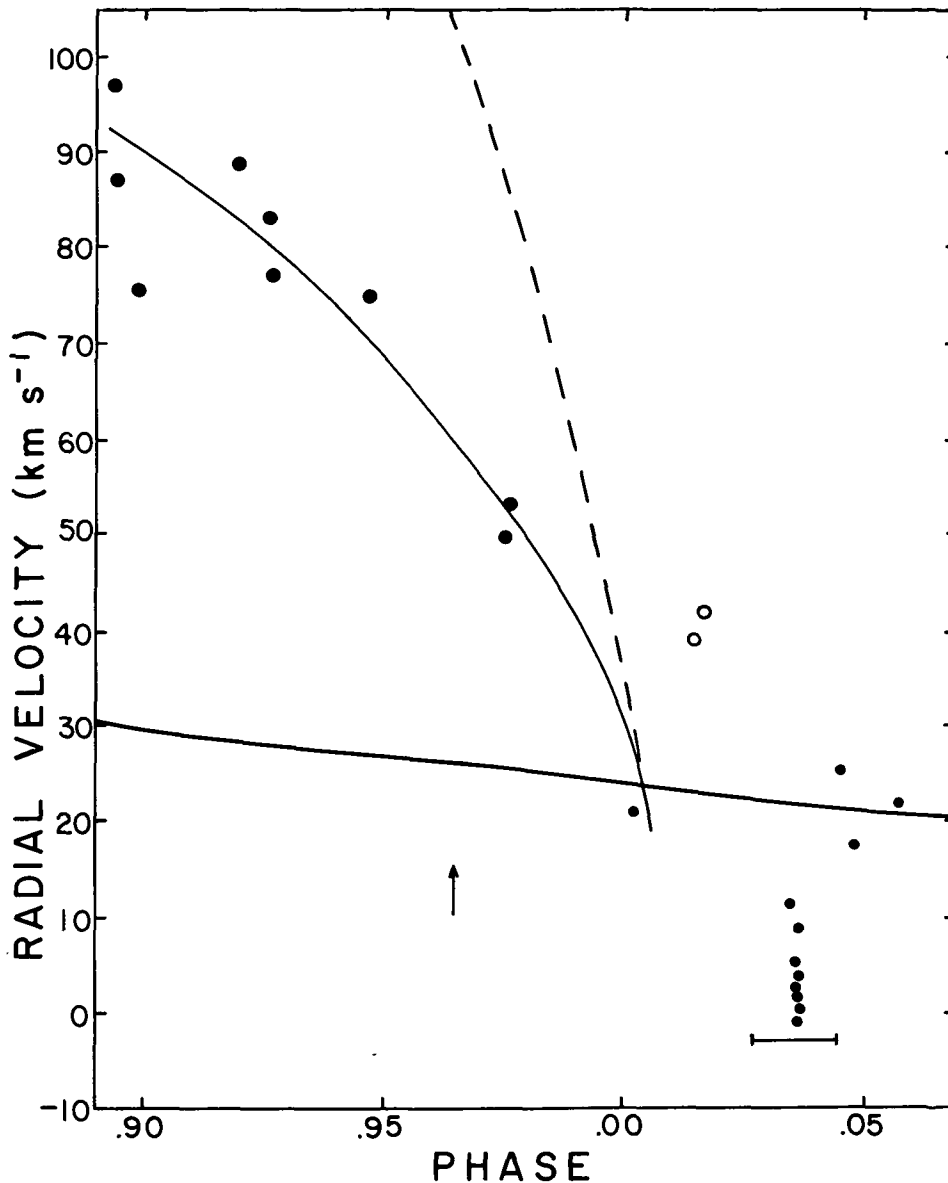


FIG. 2—Radial velocity of the  $H\beta$  gas stream line versus phase. The diagonal solid, thick line which runs from 30 to 20  $\text{km s}^{-1}$  (left to right) represents the motion of the photosphere of the primary star. The vertical arrow at phase 0.96 locates  $\Phi_s = 0.0$ . The horizontal line between  $0.03 < \phi < 0.04$  indicates the duration of the *secondary* shell phase. Thin solid and dashed lines show fit to observations and results from model calculations, respectively.

locities of the shell lines are positive with respect to the photosphere during the *primary* shell phase but negative in the *secondary* shell phase. The trend in the velocities observed throughout the two-component shell phase, readily seen in Figure 2, is discussed further in section V.

An earlier suggestion that a Balmer progression exists during the *primary* shell phase and remains constant with phase does not seem to be supported by the newer measurements (cf. Table III). However, during the *secondary* shell phase, the higher Balmer lines *do* appear to show a significantly lower velocity than does  $H\beta$  and, therefore, suggest the presence of a radial deceleration as one looks outward from the stellar photosphere along

the line of sight. The velocities measured for  $\text{He I } \lambda 3889$  appear to agree most closely with those observed for  $H\beta$ .

The sharp  $\text{Ca II K}$  line was measured to determine whether there is a cool component to the circumstellar matter. As one can readily see from Figure 3, the weak K line observed in the spectrum of HR 2142 appears to be entirely interstellar in origin.

### V. Tentative Model and Discussion

The observations presented in this paper leave little doubt that HR 2142 is a mass-transfer binary and the emission-line character of this star is a result of the mass

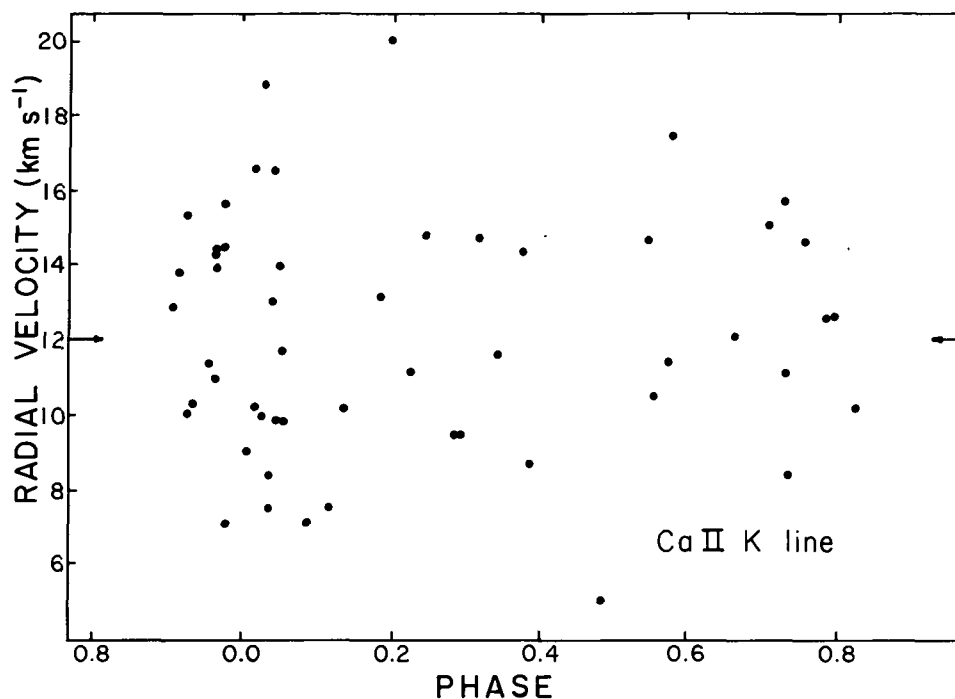


FIG. 3.—The radial velocity measured for the Ca II K line versus phase. The horizontal arrow shows the mean value from all measurements.

flow in the system. These ground-based observations allow one to refine the earlier model proposed for the system; a polar view of a suggested new model is shown in Figure 4. The orbital solution has revealed the phase for conjunction in this system and, indeed, the fact that the conjunction point is within 0.015 of the place predicted from the earlier analysis illustrates that the behavior of shell lines *can* be employed to construct a plausible model for systems which show simple periodic shell activity.

Most references quote a spectral type of B2 IV–Ve for HR 2142 but the clear presence of shallow, 100 mÅ lines of N II  $\lambda$ 3995, O II  $\lambda$ 4072, and C II  $\lambda$ 4267 observed on a microphotometer tracing of a 5.5 Å mm<sup>-1</sup> coude plate from the Lick Observatory spectrograph suggests that the photospheric temperature of this star is about 24,000 K–25,000 K. Therefore, a spectral class closer to B1–B1.5 perhaps is more representative of the star. It should be mentioned, however, that, as a result of its rapid rotation and envelope emission, HR 2142 displays one of the lowest contrast spectra observed amongst early B stars and one can readily accept an uncertainty of one subclass in its spectral type. Since plausible values for the mass and radius of a B1.5 IV–V star are 11  $M_{\odot}$  and 8  $R_{\odot}$ , respectively (Popper 1980), these will be adopted for the primary. The mass function from the orbital solution (0.007  $M_{\odot}$ ) thus implies a mass of 1.0  $M_{\odot}$  for the secondary.

Since one currently observes a high rate of mass transfer (Peters 1976), the secondary most likely fills its critical Roche surface and, therefore, has a radius of about 31

$R_{\odot}$ . A problem which remains to be solved, however, is why the spectrum of the secondary star has, to this date, never been observed. We can rule out the presence of (1) a high-temperature star ( $> 10,000$  K) because we observe the “gas stream” lines to reach an intensity near zero in the far ultraviolet and (2) a very cool object ( $< 3500$  K) since one does not observe its radiation in the infrared (Allen 1973). An object of surface temperature 4000 K–6000 K would be the most difficult to detect. According to Johnson (1966), a star in this temperature range with the above stated size should only be 1<sup>m</sup>0–1<sup>m</sup>5 fainter than the primary in the near infrared but our own spectroscopic observations at 8500 Å failed to reveal evidence of the secondary. Perhaps the extensive mass loss which is presumably occurring over a quarter of the stellar surface reduces the overall luminosity of the star.

The dimension of the system implied by the orbital solution and the assumption regarding the primary’s mass is 0.84 AU or 180  $R_{\odot}$ . Since HR 2142 does not appear to be an eclipsing system, its maximum inclination to our line of sight is 75°–80°. Such an inclination is compatible with the measured  $v \sin i$  for the primary.

The basic model shown in Figure 4 has been generated with the aid of a computer code for calculating three-body trajectories. The gas stream is the path of a test particle launched from the inner Lagrangian point,  $L_1$ . In accordance with the calculations of Lubow and Shu (1975), we have drawn the width of the gas stream to be of the order  $\epsilon$ , the ratio of the isothermal sound speed to the product of the system’s angular velocity

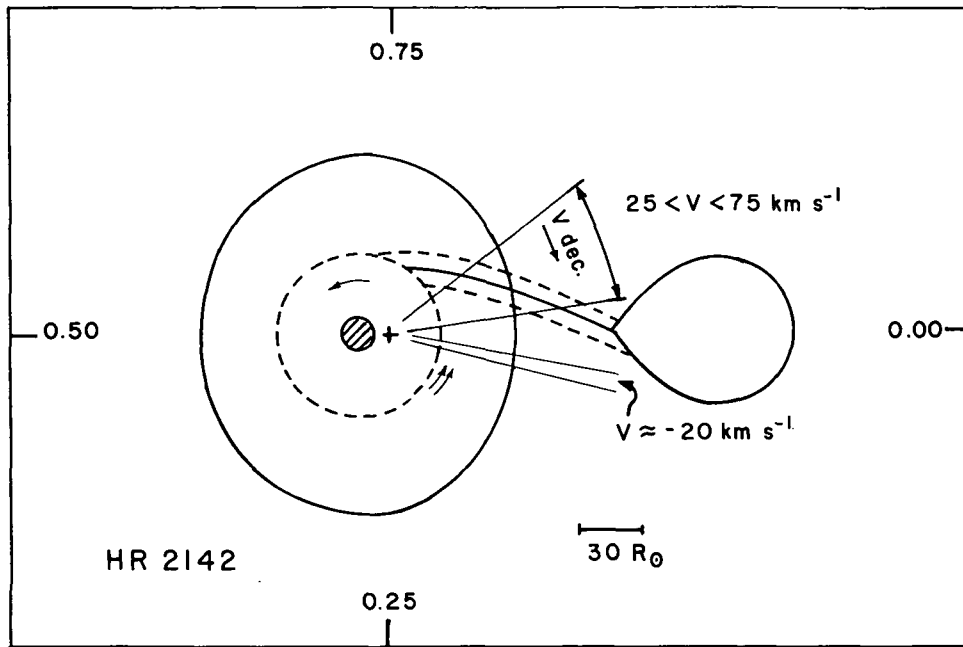


FIG. 4—Polar view of the proposed model for HR 2142, drawn to scale, based upon the analysis of the visual spectrograms discussed in this paper. The primary star ( $R \approx 8 R_{\odot}$ ) is indicated by the hatched circle while it is assumed that the secondary fills its critical Roche surface. The disk about the primary and the trajectory of the gas stream particles are discussed in the text. The wider, open triangle delineates the *primary* shell phase showing the phase interval over which the “gas stream” lines are observed; the thinner triangle indicates the extent of the *secondary* shell phase. Velocities quoted are with respect to the photosphere of the primary. Phases increase in a clockwise fashion from conjunction.

multiplied by the system’s semimajor axis. The inner disk about the primary, denoted by the dashed circle in Figure 4, shows the location of the dense disk in accordance with the computations of Lubow and Shu (1975). The outer disk, shown by the solid curve, is the outermost stable orbit. This orbit is well within the Roche surface of the primary star.

The *domain* over which the gas stream lines are observed during the *primary* shell phase is indicated by the open triangle in Figure 4. Velocities which range from 75 to 25  $\text{km s}^{-1}$  (relative to the photosphere) are seen. But our three-body calculations suggest that the observed velocities should be about a factor of two larger if the Balmer “shell” lines are formed in the gas stream (Fig. 2). Harmanec (1982) has also commented on the low velocities observed for gas stream features in Be stars. It should be kept in mind that we view the system at an angle of about  $15^\circ$  out of the plane of the orbit. What we might be observing are the effects at high latitudes of an interaction between the gas stream and the disk.

Column densities from the Balmer shell lines observed during the *primary* shell phase ( $0.95 < \phi < 0.98$ ) average  $3.0 \times 10^{14} \pm 1.0 \times 10^{14} \text{ cm}^{-2}$ . The mass flow rate toward the primary star deduced from these column densities is necessarily model dependent. If we assume that the Balmer features are formed in or near the gas stream about  $10 R_{\odot}$  from the primary (see Fig. 4) in a medium

of 12,000 K, we obtain a total hydrogen column density of  $3 \times 10^{21} \text{ cm}^{-2}$ . The ionization fraction for hydrogen was computed with the aid of the Oegerle-Polidan ionization equilibrium code (personal communication) in which photoionization in a dilute radiation field was included. Now adopting a value of  $20 R_{\odot}$  ( $2.5 R_{\odot}$ ) for the path-length,  $h$ , we conclude  $N_{\text{H}} \approx 2 \times 10^9 \text{ cm}^{-3}$  in the Balmer-line-forming region. The minimum mass flow rate implied by this density is thus  $10^{-8} M_{\odot} \text{ yr}^{-1}$  (if the gas stream is 10% He and uniform in density with a radius  $\approx \epsilon$  or  $20 R_{\odot}$ ). But, as noted above, we are only observing the high-latitude component of the mass flow which should be substantially lower in density than the center of the stream.

The *secondary* shell phase remains the most novel and confusing aspect of the HR 2142 system. The negative velocities and short duration suggest that for a brief instant in phase we view the light of the primary through some “counter streaming” matter above the orbital plane and, furthermore, the strict periodicity clearly demonstrates the remarkable stability of the line-forming region. The domain of the *secondary* shell phase is shown in Figure 4. The representation of the negative velocity matter (NVM) observed during the *secondary* shell phase differs from models previously published by the author in that only a domain is indicated since it no longer appears certain that we are observing a true counter stream. In fact, ultraviolet observations suggest



that the line formation region is located at least  $10 R_*$  from the primary star (Peters and Polidan, in preparation) and more likely in the vicinity of the secondary. The Balmer progression, which seems well established, indicates an outflow in this region which decreases with distance from the primary. He I shell features from the  $2^1S$  level (3965 Å, 5016 Å) presumably formed in a region of lower density farther away from the primary, are stronger during the *secondary* shell phase and move with H $\beta$ . The higher Balmer features observed during the *secondary* shell phase give a slightly higher column density ( $5 \times 10^{14} \text{ cm}^{-2}$ ) than observed during the *primary* shell phase. This could be explained if the line-formation region is farther from the primary star where the fraction of ionized hydrogen is lower. An alternative to a counter stream is the possibility that the matter producing the *secondary* shell phase is located in an extended atmosphere about the secondary. But the observed outflow velocities would suggest that the secondary is rotating supersynchronously and it would be difficult to explain the Balmer progression with such a model.

Phase dependent ultraviolet observations have been obtained of HR 2142 with the *IUE* and *Copernicus* satellites. The results from these investigations reveal additional information about this remarkable system (Peters 1980; Peters and Polidan 1982) and the full analyses will be published shortly.

I am most grateful to D. M. Popper and M. Plavec for generously obtaining spectrograms of this long-period system over a number of years, and thank the director of

Lick Observatory for allocation of telescope time. I wish to thank J. B. Hutchings for measuring selected spectrograms in order to assess the suitability of ARCTURUS for this project and for securing permission for my visit to DAO. I also thank P. B. Etzel for instruction in the use of the newest version of the UCLA Spectroscopic Binary Orbit Program. Finally, I acknowledge numerous on-going discussions on HR 2142 with R. S. Polidan and thank him for computing the three-body trajectories and for the use of his ionization code prior to publication. This project has been supported, in part, by NASA grants NSG 5056, NSG 5356, and NAG 5-126.

#### REFERENCES

- Allen, D. A. 1973, *M.N.R.A.S.* 161, 157.  
 Harmanec, P. 1982, in *Be Stars, I.A.U. Symposium No. 98*, M. Jaschek and H. G. Groth, eds. (Dordrecht: Reidel), p. 279.  
 Johnson, H. L. 1966, *Ann. Rev. Astr. and Ap.* 4, 193.  
 Lubow, S. H., and Shu, F. H. 1975, *Ap. J.* 198, 383.  
 Peters, G. J. 1971, *Ap. J. (Letters)* 163, L107.  
 ——— 1972, *Pub. A.S.P.* 84, 334.  
 ——— 1976, in *Be and Shell Stars, I.A.U. Symposium 70*, A. Slettebak, ed. (Dordrecht: Reidel), p. 417.  
 ——— 1981, in *The Universe at Ultraviolet Wavelengths*, NASA Conf. Pub. No. 2171, 157.  
 Peters, G. J., and Polidan, R. S. 1973, in *Extended Atmospheres and Circumstellar Matter in Spectroscopic Binary Systems I.A.U. Symposium No. 51*, A. H. Batten, ed. (Dordrecht: Reidel), p. 174.  
 ——— 1982, in *Be Stars, I.A.U. Symposium No. 98*, M. Jaschek and H. G. Groth, eds. (Dordrecht: Reidel), p. 405.  
 Popper, D. M. 1980, *Ann. Rev. Astr. and Ap.* 18, 115.  
 Slettebak, A. 1976, in *Be and Shell Stars, I.A.U. Symposium No. 70*, A. Slettebak, ed. (Dordrecht: Reidel), p. 123.  
 ——— 1982, *Ap. J. Suppl.* 50, 55.

# ON THE PRESENCE OF O I $\lambda$ 1302 EMISSION IN Be STARS

W. R. OECERLE

Princeton University Observatory, Peyton Hall, Princeton, New Jersey 08544

G. J. PETERS\*†

Department of Astronomy, University of Southern California, University Park, Los Angeles, California 90007

AND

R. S. POLIDAN†

Princeton University Observatory, Peyton Hall, Princeton, New Jersey 08544

Received 1982 July 22, revised 1982 November 2

In many Be stars, the O I  $\lambda$ 8446 line is present as a strong emission line, which is generally attributed to Lyman- $\beta$  fluorescence. In the fluorescence process, if simple cascade follows the excitation, one 8446 Å photon and one 1302 Å, 1305 Å, or 1306 Å photon will be emitted. However, emission in the UV O I triplet was not obviously present in any previous spectra of Be stars taken with *Copernicus* or *IUE*. Using plausible models for Be star disks, we have calculated the expected strength of the O I  $\lambda$ 1302 emission line for a few Be stars that display strong O I  $\lambda$ 8446 emission. We find that even in optically thin cases the relative intensity of the O I  $\lambda$ 1302 emission line will be modest because of the large continuum flux in the ultraviolet. In an optically thick case, which describes most Be star envelopes, destruction of the O I  $\lambda$ 1302 line by various atomic processes will reduce the strength of the emission line below detectable limits.

**Key words:** Be stars—emission lines—IR observations—UV observations

## I. Introduction

The O I  $\lambda$ 8446 transition ( $3s^3S^0-3p^3P$ ,  $\lambda\lambda$ 8446.25, 8446.36, and 8446.76) is present as a strong emission line in many Be stars. Bowen (1947) suggested that the anomalous strength of this line is due to the overpopulation of the  $3d^3D^0$  state of O I by the absorption of  $L\beta$  photons (Fig. 1). In this fluorescence process, the absorption of a  $L\beta$  photon is followed by the emission of one 11,287 Å photon, one 8446 Å photon, and one resonance (1302, 1305, or 1306) photon. Therefore, Be stars which display O I  $\lambda$ 8446 in emission should also be expected to have the UV O I triplet ( $\lambda\lambda$ 1302.17, 1304.86, and 1306.02) in emission.

Peters (1976b) scanned the O I UV triplet region in  $\mu$  Centauri,  $\nu$  Cygni, and  $\phi$  Persei with *Copernicus*, but found no obvious evidence of O I emission. In a recent study of the ultraviolet spectrum of  $\phi$  Per with *IUE*, Kitchin (1982) remarks that the lack of O I  $\lambda$ 1302 emission is "puzzling" because the line "... should be easily visible."

The purpose of this study is to explain the absence of the UV O I emission in terms of a plausible model for the Be star circumstellar disk.

## II. Observations

Ultraviolet observations of Be stars with strong O I  $\lambda$ 8446 emission were obtained with the *Copernicus* and

the *IUE* spacecraft. The *Copernicus* data were taken with the U2 spectrometer (resolution  $\sim 0.2$  Å) in 1979. Additional UV observations were made with the *IUE* (resolution  $\sim 0.13$  Å) between 1979 and 1982 by one of the authors (G.I.P.) as part of a general study of Be stars. Infrared observations were obtained at Lick Observatory and Kitt Peak National Observatory by two of the authors (G.I.P. and R.S.P.) as part of an ongoing study of the infrared region in Be stars. The Lick spectrograms,

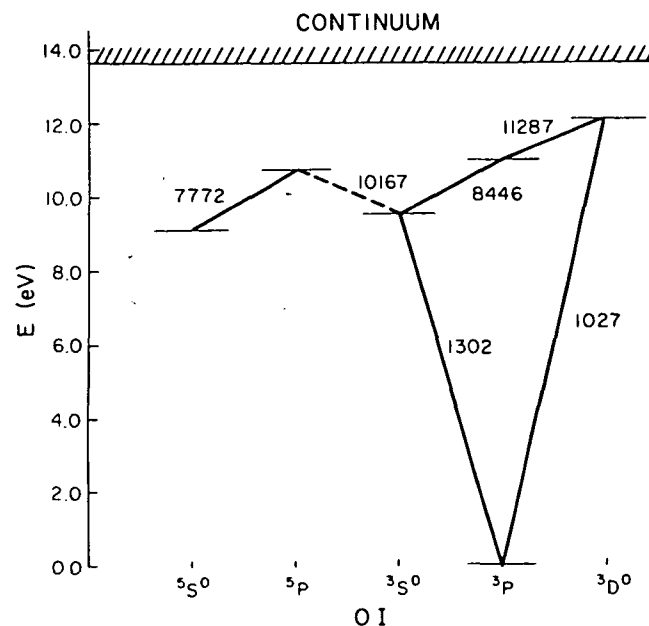


FIG. 1—Partial Grotrian diagram for O I.

\*Guest Observer, *International Ultraviolet Explorer*.

†Guest Astronomer, Kitt Peak National Observatory, operated by AURA, Inc., under contract with the National Science Foundation.

taken between 1974 and 1976 using the coudé Varo image-tube system with the 3-m Shane Telescope and the 0.6-m coudé auxiliary telescope, were baked IIIa-J, 127-04, or 103a-D plates at a dispersion of  $23 \text{ Å mm}^{-1}$ , widened to 0.6 mm. The KPNO spectrograms, taken in 1981 and 1982 using the coudé CCD in conjunction with the 0.9-m coudé feed telescope, are at a dispersion of  $15 \text{ Å mm}^{-1}$  (resolution: 1981,  $\sim 0.2 \text{ Å}$ ; 1982,  $\sim 0.4 \text{ Å}$ ).

The observed stars all display rather strong O I  $\lambda 8446$  emission, but in no case was significant O I  $\lambda 1302$  emission detected. Table I summarizes the observations. The first three columns of Table I list, respectively, the star, its spectral type, and  $v \sin i$ . The fourth column lists the computed continuum flux ratio,  $I_c(8446)/I_c(1302)$ , for each star. These values were obtained through interpolation in the Kurucz (1979) grid of model atmospheres. The Kurucz  $\lambda 8450$  flux point was used as the  $\lambda 8446$  continuum flux and the Kurucz  $\lambda 1312$  flux point, modified to account for the observed additional line blocking in the O I region, was used as the  $\lambda 1302$  continuum flux. Stellar effective temperatures were taken from Peters (1976a) for all stars except 48 Mibrae and  $\kappa$  Draconis. For these two stars effective temperatures were estimated from published spectral types. The fifth and sixth columns list, respectively, the observed  $\lambda 8446$  emis-

sion intensity and the two sigma upper limit to the  $\lambda 1302$  emission intensity. The results listed for the  $\lambda 1302$  emission are consistent with previous investigations.

### III. Discussion

In order to understand these observations, we now consider various models for the circumstellar gas. Initially, it is instructive to construct a simple optically thin (in O I  $\lambda 1302$ ) model. In this gas, each  $\lambda 8446$  photon will give rise to either a  $\lambda 1302$ , 1305, or 1306 photon that will escape the disk. The relative strengths of the three resonance lines will be specified by the relative A values. These are given by Haisch et al. (1977) and are in the approximate ratio of 5:3:1 for 1302: 1305: 1306. Thus, for the stars in Table I, the peak intensity of one of the UV O I triplet lines can be computed from the observed  $\lambda 8446$  strength, the relative continuum strength and the branching ratio. Specifically, we find

$$\frac{I_L(\lambda_i)}{I_c(\lambda_i)} = 1 + \frac{A_i}{\sum A_i} \left( \frac{8446}{\lambda_i} \right)^2 \times \left( \frac{I_c(8446)}{I_c(\lambda_i)} \right) \left( \frac{I_L(8446)}{I_c(8446)} - 1 \right), \quad (1)$$

where  $\lambda_i = 1302, 1305, \text{ or } 1306$ ,  $I_L(\lambda)$  is the line peak

TABLE I

OI EMISSION LINE STRENGTHS

Star	SP <sup>1</sup>	$v \sin i$ <sup>1</sup>	$(I_c(8446)/I_c(1302))^2$	$(I(8446)/I_c(8446))^3_{\text{obs}}$	$(I(1302)/I_c(1302))^3_{\text{obs}}$	$(I(1302)/I_c(1302))^4_{\text{pre}}$
$\chi$ Oph	B1.5V	140	$4.52 \times 10^{-3}$	2.00 L	$\leq 1.08$ C	1.11
66 Oph	B2IV-V	240	$5.41 \times 10^{-3}$	1.50 K	$\leq 1.2$ I	1.06
$\nu$ Cyg	B2.5V	180	$5.26 \times 10^{-3}$	1.3 L	$\leq 1.2$ I	1.04
HR 2825	B3V	$\leq 40$	$1.19 \times 10^{-2}$	1.3 L	$\leq 1.1$ I	1.08
$\epsilon$ Cap	B3:III	250	$9.37 \times 10^{-3}$	1.2 L	$\leq 1.1$ I	1.04
48 Lib	B3:IV:	400	$1.87 \times 10^{-2}$	1.5 L	$\leq 1.10$ C	1.22
48 Per	B4V	200	$1.81 \times 10^{-2}$	1.3 L	$\leq 1.2$ I	1.13
$\beta$ Psc	B5V	100	$2.41 \times 10^{-2}$	1.27 K	$\leq 1.3$ I	1.15
$\kappa$ Dra	B5III	200	$3.22 \times 10^{-2}$	1.20 K	$\leq 1.2$ I	1.15
$\psi$ Per	B5III	280	$1.74 \times 10^{-2}$	1.5 L	$\leq 1.07$ C	1.20

<sup>1</sup> Slettebak (1982)

<sup>2</sup> From Kurucz (1979), see text

<sup>3</sup> Key: L = Lick, K = Kitt Peak, C = Copernicus, I = IUE

<sup>4</sup> From Equation 1

intensity, and,  $I_c(\lambda)$  is the continuum intensity at the line. The predicted line peak intensities for the  $\lambda 1302$  line in the observed stars are listed in the last column of Table I. Note that the peak intensities are quite small. The principal reason for this is the strong stellar ultraviolet continuum.

In his recent study of  $\phi$  Per, Kitchin (1982) calculates that the O I  $\lambda 1302$  emission line should have an intensity of about three times the continuum and is puzzled as to why the line is not present. Based on our calculations for  $\phi$  Per, we suggest that Kitchin has substantially overestimated the expected strength of the O I  $\lambda 1302$  emission line. Our results are in agreement with those computed by Peters (1976b).

We note that for some of the stars in Table I the expected emission strength is greater than the observed upper limits, and should be detectable. However, those predictions were based on the assumption that the gas was optically thin. This assumption is probably not valid for the majority of stars observed. Thus, we now must consider other atomic processes that could alter the emission strength.

True absorption occurs when an atom in the  $3s^3S^0$  level is collisionally de-excited to the ground state, thereby destroying the resonance-line photon. The ratio of the radiative de-excitation rate to the collision de-excitation rate from the  $3s^3S^0$  level is  $A_{21}/N_e\Omega_{21} \approx 10^{17}/N_e$  where we have used atomic rates from Haisch et al. (1977). Other sources of  $\lambda 1302$  photon destruction include collisional and radiative ionization from the  $3s^3S^0$  level, which will be overpopulated relative to LTE conditions. Another possible photon sink is the partially forbidden transition  $3s^3S^0 - 3p^5P$  (multiplet 3.02,  $\lambda\lambda 10167.252, 10169.347$ ). A search of published atomic parameters failed to find a transition probability or collision strength for the transition. Values typical of intercombination transitions have been assumed. Investigation of the sources of photon destruction (collisional de-excitation, ionization, and excitation out of the triplet series) suggests that the total destruction rate is about ten times the collisional de-excitation rate from the  $3s^3S^0$  level. Thus, for the  $3s^3S^0$  level the ratio of the radiative de-excitation rate to the total photon destruction rate in the level is approximately  $10^{16}/N_e$ . Therefore, in a typical Be star envelope with  $N_e \sim 10^{12} \text{ cm}^{-3}$ , an O I resonance-line photon will be scattered  $\sim 10^4$  times before being destroyed. The total scattering optical depth at line center is (cf. Spitzer 1978)

$$\tau_0 = \frac{1.497 \times 10^{-2}}{b} \lambda f_{12} n_1 f, \quad (2)$$

where  $b$  is the velocity spread parameter ( $3.6 \times 10^5 \text{ cm s}^{-1}$  for oxygen),  $\lambda$  is the wavelength,  $f$  is the oscillator strength,  $n_1$  is the number density of atoms in the appro-

priate level, and  $f$  is the path length. If we assume a total hydrogen density in the envelope of  $10^{12} \text{ cm}^{-3}$ , ionization equilibrium calculations (including radiative processes, dielectronic recombination, and charge exchange) yield O I ionization fractions between  $10^{-4}$  and  $10^0$  for the stars in Table I. This implies values of  $n_1$  between  $10^5$  and  $10^9 \text{ cm}^{-3}$ , and with path lengths  $\sim 10^{12} \text{ cm}$  gives a  $\tau_0$  of between  $10^3$  and  $10^7$ . Thus, it appears that in most cases the resonance-line photon will be scattered enough that one of the possible destruction mechanism will remove the photon.

We should point out here that opacity broadening ( $\propto (n \tau_0)^{1/2}$ ) of the resonance lines will significantly effect their observability. Line center optical depths of  $10^3$  to  $10^7$  will result in line widths of 2.6 to 4.0 times larger than that of the optically thin case. This will further decrease the already small line peak intensities.

In the previous discussion we pointed out the possibility that an O I atom in the  $3s^3S^0$  state may be excited (radiatively or collisionally) and move to the  $3p^5P$  state. After this process, a subsequent radiative decay to the  $3p^5S^0$  level will occur emitting a  $\lambda 7772$  photon (see Fig. 1). Although we cannot state with any assurance the probability of this occurring, cross-coupling will result in an overpopulation of the  $5S^0$  and  $5P$  states. This could help explain the "anomalous" behavior of O I  $\lambda 7772$ , which has been observed in emission in Be stars with strong O I  $\lambda 8446$  emission even though its lower level ( $5S^0$ ) is metastable (Polidan and Peters 1976). This mechanism for overpopulating the  $3p^5S^0$  level could also help resolve some of the difficulties Haisch et al. (1977) encountered in matching their calculated quintet line strengths with the observations for Arcturus. Any evaluation of the importance of this triplet-quintet link must await determination of the pertinent atomic parameters. If these parameters were available, a detailed solution of the O I atom could be made and the effect of the triplet-quintet cross-coupling on line strengths estimated.

One final possible influence on the observed emission-line strength is the geometry of the Be star envelope. Since the optical depth to line scattering depends on the population in the lower level of the transition, the optical depth in O I  $\lambda 8446$  will be much lower than in O I  $\lambda 1302$ . Consequently, if Be envelopes are flattened, stars seen equator-on will scatter more resonance-line ( $\lambda 1302$ ) photons out of our line-of-sight than subordinate-line ( $\lambda 8446$ ) photons. This will reduce the expected resonance-line strength and explain the observations. However, for stars seen pole-on, the flattened disk will preferentially scatter resonance photons perpendicular to the plane, into our line-of-sight, increasing the emission strength. This process would work only if the O I emitting region is highly flattened, otherwise the photon destruction processes discussed above would dominate.

However, as one can see from Table I, the stars with low values of  $v \sin i$  do not show any significant enhancement of O I emission relative to the high  $v \sin i$  stars.

#### IV. Summary

Given the unusual strength of O I  $\lambda 8446$  in Be stars, we have shown that even in the most optimistic case (optically thin), O I  $\lambda 1302$  emission is not expected to be very strong relative to the local continuum. Furthermore, for more realistic models, we find that resonance-line scattering should decrease the emission below detectable limits in most Be stars. It may be possible to detect resonance emission in pole-on Be stars if the scale height of the O I emitting region is small enough to allow the escape of resonance photons in this direction. Detection of emission in early-type Be stars is difficult primarily because of the large UV continuum flux. These considerations indicate that detection of O I  $\lambda 1302$  emission should be easiest in late-B, pole-on Be stars.

The authors gratefully acknowledge the support of NASA Grants NAS5-23576 (W.R.O. and R.S.P.) and NSC

5422 (G.I.P.) in this investigation. G.I.P. and R.S.P. also wish to acknowledge support of the NSF Grant to Popper and Plavec and the help of the staffs of Lick Observatory and Kitt Peak National Observatory in obtaining the infrared observations. The authors also wish to thank the *Copernicus* and *IUE* staffs for their help and J. B. Rogerson, Jr. and the referee for helpful discussion and comments.

#### REFERENCES

- Bowen, I. S. 1947, *Pub. A.S.P.* 59, 196.  
 Haisch, B. M., Linsky, J. L., Weinstein, A., and Shine, R. A. 1977, *Ap. J.* 214, 785.  
 Kitchin, C. R. 1982, *M.N.R.A.S.* 198, 457.  
 Kurucz, R. L. 1979, *Ap. J. Suppl.* 40, 1.  
 Peters, G. J. 1976a, in *Be and Shell Stars, I.A.U. Symposium No. 70*, A. Slettebak, ed. (Dordrecht: Reidel), p. 69.  
 ——— 1976b, in *Be and Shell Stars, I.A.U. Symposium No. 70*, A. Slettebak, ed. (Dordrecht: Reidel), p. 209.  
 Polidan, R. S., and Peters, G. J. 1976, in *Be and Shell Stars, I.A.U. Symposium No. 70*, A. Slettebak, ed. (Dordrecht: Reidel), p. 59.  
 Slettebak, A. 1982, *Ap. J. Suppl.* 50, 55.  
 Spitzer, L., Jr. 1978, *Physical Processes in the Interstellar Medium* (New York: Wiley), p. 53.